

# NA49 AND NA61/SHINE EXPERIMENTS: RESULTS AND PERSPECTIVES\*

KATARZYNA GREBIESZKOW

for the NA49 and the NA61 Collaborations

Faculty of Physics, Warsaw University of Technology  
Koszykowa 75, 00-662 Warsaw, Poland

*(Received December 1, 2009)*

The Super Proton Synchrotron (SPS) covers one of the most interesting regions of the QCD phase diagram ( $T - \mu_B$ ). On the one hand, there are indications that the energy threshold for deconfinement is reached already at low SPS energies. On the other hand, theoretical calculations locate the QCD critical end-point at energies accessible at the SPS. In this paper the NA49 signatures of the onset of deconfinement are presented. Results are shown on pion production, the kaon to pion ratio, slopes of transverse mass spectra (“temperature”), and event-by-event particle ratio fluctuations *versus* collision energy, for central Pb + Pb interactions. Next, we show possible indications of the critical point in event-by-event mean transverse momentum and multiplicity fluctuations. Finally, we discuss the future ion program of the NA61/SHINE experiment (energy scan with light ions).

PACS numbers: 25.75.Ag, 25.75.Gz, 25.75.Dw, 25.75.Nq

## 1. Introduction

It is a well established fact that matter exists in different states. For strongly interacting matter at least three are expected: normal nuclear matter (liquid), hadron gas (HG), and a system of deconfined quarks and gluons (eventually the quark–gluon plasma). One of the most important goals of high-energy heavy-ion collisions is to establish the phase diagram of strongly interacting matter by finding the possible phase boundaries and critical points. In principle, we want to produce the quark–gluon plasma (QGP) and analyze its properties and the transition between QGP and HG.

---

\* Presented at the XXXI Mazurian Lakes Conference on Physics, Piaski, Poland, August 30–September 6, 2009.

The phase diagram of strongly interacting matter (Fig. 1) is most often presented in terms of temperature  $T$  and baryochemical potential  $\mu_B$ . It is believed that for large values of  $\mu_B$  the phase transition is of the first order (gray band) and for low  $\mu_B$  values a rapid but continuous transition (crossover). A critical point of second order (CP) separates those two regions. The open points in Fig. 1 are hypothetical locations reached by the high-density matter droplet after dissipation of the energy of the incident nucleons from where the evolution of the expanding and cooling fireball starts. The closed symbols are chemical freezeout points [1] (chemical composition fixed, the end of inelastic interactions). The fireball then expands further until thermal (kinetic) freeze-out takes place (particle momenta are fixed).

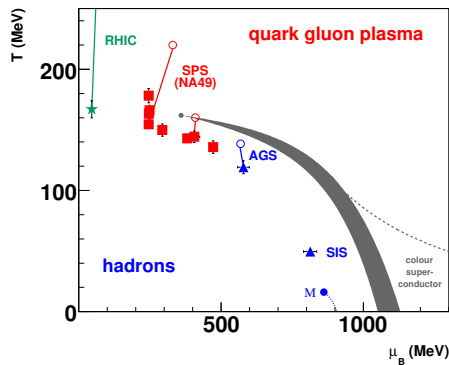


Fig. 1. QCD phase diagram.

The Super Proton Synchrotron (SPS) covers one of the most interesting regions of the QCD phase diagram ( $T - \mu_B$ ). On the one hand, it is expected that the energy threshold for deconfinement is reached already at low SPS energies (see the open point hitting the transition line in Fig. 1). On the other hand, lattice QCD calculations locate the critical point of strongly interacting matter in the SPS energy range [2].

## 2. NA49 experiment

NA49 [3], operating in 1994–2002, was one of the fixed target heavy-ion experiments at the CERN SPS. The main components of the detector were four large volume time projection chambers (TPC). The Vertex TPCs (VTPC-1 and VTPC-2), were located in the magnetic field of two superconducting dipole magnets. Two other TPCs (MTPC-L and MTPC-R) were positioned downstream of the magnets symmetrically to the beam line. The NA49 TPCs allowed precise measurements of particle momenta  $p$  with a resolution of  $\sigma(p)/p^2 \cong (0.3 - 7) \times 10^{-4} (\text{GeV}/c)^{-1}$ . A precise measurement of specific energy loss ( $dE/dx$ ) in the region of relativistic rise

was possible in the TPCs. Time of Flight (ToF) walls supplemented particle identification close to mid-rapidity. The typical  $dE/dx$  resolution was  $\sigma(dE/dx)/\langle dE/dx \rangle \approx 0.04$ , the typical ToF resolution  $\sigma(\text{ToF}) \approx 60$  ps, and invariant mass resolution (for identification of particles via decay topology) was  $\sigma(m_{\text{inv}}) \approx 5$  MeV. The centrality of nuclear collisions was selected via measurement of the energy of the projectile spectator nucleons in the Forward Calorimeter. The NA49 acceptance covers the forward hemisphere, but because of the symmetry of nucleus + nucleus ( $A + A$ ) collisions this nevertheless allows to extract  $4\pi$  integrated multiplicities.

### 3. NA49 evidence for the onset of deconfinement

#### 3.1. Kink, horn, step and SMES

In 2002 the NA49 experiment completed the SPS energy scan of central Pb + Pb collisions. This program was originally motivated by predictions of the Statistical Model of the Early Stage (SMES) [4] assuming that the energy threshold for deconfinement (the lowest energy sufficient to create a partonic system) is located at low SPS energies. Several structures were expected within SMES: the kink in pion production (due to increased entropy production), the horn in the strangeness to entropy ratio, and the step in the inverse slope parameter of transverse momentum spectra (constant temperature and pressure in a mixed phase).

Figure 2 shows production of charged pions (the total entropy is carried mainly by pions<sup>1</sup>)  $\langle \pi \rangle = 1.5(\langle \pi^+ \rangle + \langle \pi^- \rangle)$  normalized to the number of wounded nucleons *versus* Fermi variable  $F$  ( $F \approx (s_{NN})^{1/4}$ ). In SMES, this ratio is proportional to the effective number of degrees of freedom (NDF) to the power of 1/4. For central  $A + A$  collisions (Pb + Pb for SPS or Au + Au for AGS and RHIC) a change of slope around  $30 A$  GeV is visible (slope in  $A + A$  increases from  $\approx 1$  (AGS) to  $\approx 1.3$  (top SPS + RHIC) — consistent with increase by a factor of 3 in NDF). Such an increase is not observed for  $p + p(\bar{p})$  reactions. The increase in NDF, when going from hadron gas to QGP, may be interpreted as a consequence of the activation of partonic degrees of freedom.

Figure 3 (left) presents the  $\langle K^+ \rangle / \langle \pi^+ \rangle$  ratio in full phase space ( $4\pi$ ) *versus* energy. In SMES, the ratio is proportional to strangeness/entropy densities. Results for  $A + A$  are very different from the results for  $p + p$  and show a sharp peak in  $\langle K^+ \rangle / \langle \pi^+ \rangle$  at  $30 A$  GeV. This peak is even more pronounced at mid-rapidity (see [5]). Recently, these intriguing NA49 results on pion and kaon yields (at mid-rapidity) were confirmed at  $\sqrt{s_{NN}} = 9.2$  GeV

<sup>1</sup> In SMES the total entropy and the total strangeness are the same before and after hadronization (the entropy cannot decrease during the transition from QGP to hadron gas), therefore pions measure the early stage entropy.

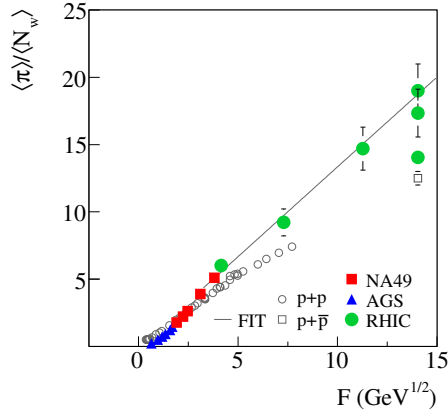


Fig. 2. Energy ( $F$ ) dependence of the mean pion multiplicity per wounded nucleon [5] in full phase space ( $4\pi$ ).

and 19.6 GeV by the STAR experiment [6]. The string hadronic models (curves in Fig. 3 (left)) do not reproduce the data. The hadron gas model (HGM) [7] using a parameterization of the energy dependence  $T_{\text{ch}}$  and  $\mu_B$  based on fits to hadron yields produces a broad maximum in the  $\langle K^+ \rangle / \langle \pi^+ \rangle$  ratio as a consequence of saturating  $T_{\text{ch}}$  and decreasing  $\mu_B$  with increasing energy (limiting temperature reached somewhere at the SPS). However, this version of the model overestimates the relative kaon yields from 30 A GeV on. The latest extension of the HGM [8] yields and improves fit of the energy dependence  $\langle K^+ \rangle / \langle \pi^+ \rangle$  by inclusion of unmeasured(!) higher-mass resonances (up to 3 GeV) in the model hadron spectrum (see conference slides or [8]).

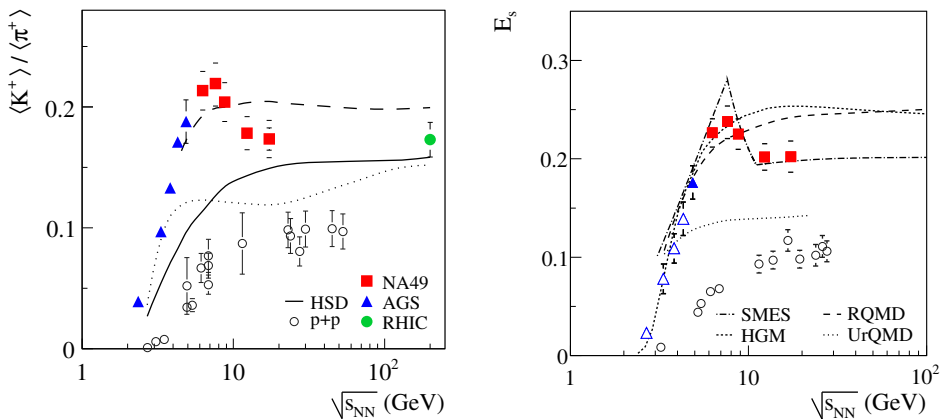


Fig. 3. Left: Energy dependence of the  $\langle K^+ \rangle / \langle \pi^+ \rangle$  ratio in full phase space ( $4\pi$ ). Right:  $E_s$  measure of strangeness to entropy ratio *versus* energy in  $4\pi$  [5].

The measure which much better reflects the total strangeness to entropy ratio in the SPS energy range is  $E_s = (\langle K \rangle + \langle \Lambda \rangle) / \langle \pi \rangle$ , proposed in Ref. [4], and calculated from  $\pi$ ,  $K$ , and  $\Lambda$  yields in  $4\pi$  acceptance. The  $E_s$  ratio can be directly and quantitatively compared to SMES predictions. Figure 3 (right) shows a distinct peak in  $E_s$  at 30 A GeV. This behavior is described (predicted) only by the model assuming a phase transition (*i.e.* SMES), where the maximum, called ‘horn’, is the result of the decrease of strangeness carrier masses in the QGP ( $m_s < m_{\Lambda, K, \dots}$ ) and the change in the number of degrees of freedom when reaching the deconfined state.

Figure 4 presents inverse slope parameters ( $T$ ) of transverse mass spectra<sup>2</sup> of positively and negatively charged kaons. For  $A + A$  data one can see a strong rise at AGS, plateau at SPS, and rise towards RHIC energies. Such structure is not observed for  $p + p$  collisions. The plateau is consistent with constant temperature and pressure in the mixed phase (latent heat) [9]. In fact, this structure strongly resembles the behavior of water, where a plateau can be observed in the temperature when heat is added. Models without phase transition do not reproduce the  $A + A$  data, but a hydrodynamical model incorporating a deconfinement phase transition at SPS energies [10] describes the results in Fig. 4 quite well. The step-like feature is also present in the energy dependence of  $m_T - m$  of protons and pions (see conference slides or [5]).

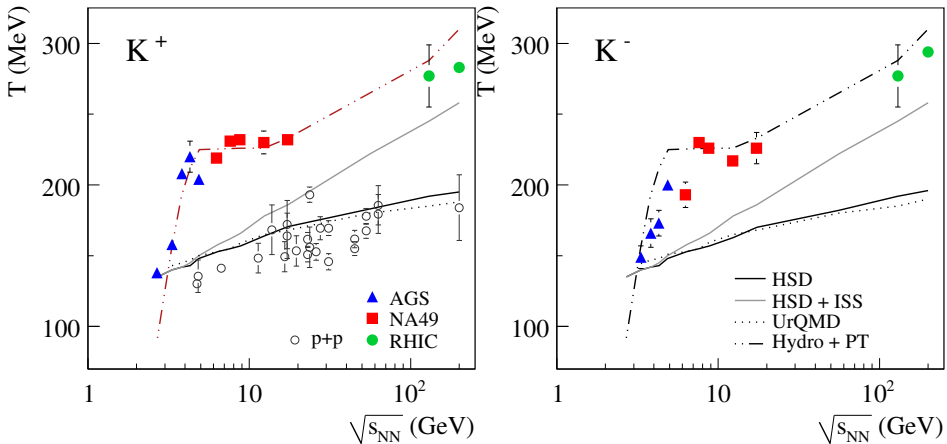


Fig. 4. Energy dependence of the inverse slope parameter  $T$  of the transverse mass spectra of  $K^+$  and  $K^-$  mesons [5].

<sup>2</sup> Transverse mass spectra were parametrized by  $dn/(m_T dm_T) = C \exp(-m_T/T)$ ; fits were done close to mid-rapidity.

### 3.2. Event-by-event particle ratio fluctuations

Hadron ratios characterize the chemical composition of the fireball and are not affected by hadronic re-interaction when looking at conserved quantities such as baryon number, strangeness. We expect a change of particle (*e.g.* strangeness) production properties close to the phase transition. In principle, two distinct event classes (with/without QGP) or the mixed phase (coexistence region of hadronic and partonic matter for 1st order phase transition) may be reflected in larger event-by-event fluctuations.

The NA49 experiment used  $\sigma_{\text{dyn}}$  [11] to quantify event-by-event particle ratio fluctuations.  $\sigma_{\text{dyn}}$  measures the difference between widths of particle ratio distributions for data and for artificially produced mixed events, where only statistical fluctuations are present. Figure 5 (left) shows that the dynamical fluctuations in the  $K/\pi$  ratio are positive. One observes a step rise towards low SPS energies but no significant change from top SPS to RHIC energies. The rise towards low energies is not reproduced by the UrQMD transport model (there is no significant acceptance dependence). The HSD transport model catches the trend but overpredicts the data at high SPS energies. Dynamical fluctuations of the  $K/p$  ratio (Fig. 5 (right)) exhibit two sign changes: a positive plateau at RHIC energies changes to a negative plateau at higher SPS energies, followed by a jump to positive value at the lowest SPS energy (20 A GeV). High energy SPS and RHIC data are reproduced by the UrQMD model, however the jump at 20 A GeV is not described (this jump between SPS and RHIC is not due to acceptance). The values of dynamical event-by-event fluctuations of the  $p/\pi$  ratio (see conference slides or [11]) are negative (both at SPS and at RHIC energies) and can be reproduced by the UrQMD model (understood in terms of baryon resonance decays) in the SPS energy range.

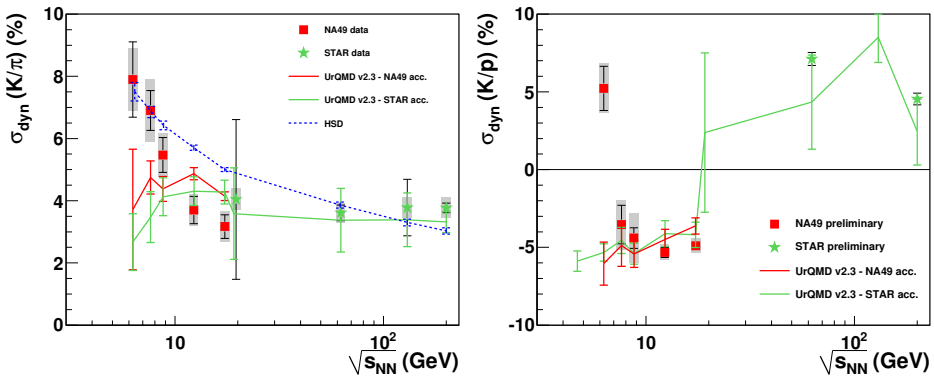


Fig. 5. Energy dependence of dynamical  $K/\pi$  (left) and  $K/p$  (right) fluctuations for 3.5% most central Pb + Pb (NA49) and for Au + Au interactions (STAR) [11].

#### 4. NA49 indications for the critical point

Lattice QCD calculations locate the QCD critical point at energies accessible at the CERN SPS [2]. In “normal” liquids (including water) the critical point can be rather easily detected via the critical opalescence phenomenon (scattering of light on critical long wavelength density fluctuations). Over the past years several experimental observables were proposed to look for the CP in heavy ion collisions. Among them are fluctuations of mean transverse momentum and multiplicity [12], pion pair (sigma mode) intermittency, elliptic flow of baryons and mesons, and transverse mass spectra of baryons and anti-baryons [13]. One should also note that for strongly interacting matter the maximum effect of the CP is expected when the freeze-out happens near the critical point.

The position of the chemical freeze-out point in the  $(T - \mu_B)$  diagram can be varied by changing the energy and the size of the colliding system as presented in Fig. 6. Therefore, we analyzed in NA49 the energy dependence of the proposed CP sensitive observables for central Pb + Pb collisions (beam energies 20 A–158 A GeV), and their system size dependence ( $p + p$ , C + C, Si + Si, and Pb + Pb) at the highest SPS energy. Figure 6 shows  $CP_1$  and  $CP_2$  that were considered in NA49 as possible locations of the critical point:  $CP_1$  with  $\mu_B$  from lattice QCD calculations [2] and  $T$  on the empirical freeze-out line;  $CP_2$  as the chemical freeze-out point of  $p + p$  reactions at 158 A GeV (assuming that this freeze-out point may be located on the phase transition line).

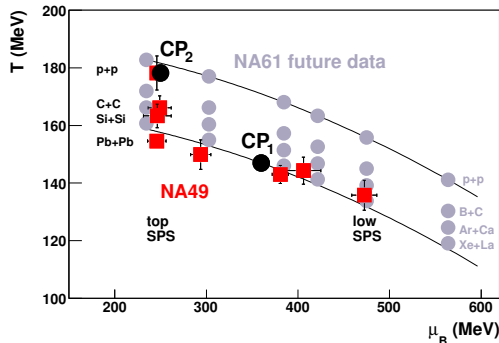


Fig. 6. Chemical freeze-out points in NA49 (squares) and those expected in NA61 (circles). See the text for details.

##### 4.1. Average $p_T$ and multiplicity fluctuations

At the critical point enlarged fluctuations of multiplicity and mean transverse momentum are expected [12]. In NA49 we used the  $\Phi_{p_T}$  fluctuation measure [14, 15] and the scaled variance  $\omega$  of multiplicity distribution [16, 17]

to study  $p_T$  and  $N$  fluctuations, respectively. For a system of independently emitted particles (no inter-particle correlations)  $\Phi_{p_T}$  is equal to zero. For a Poisson multiplicity distribution  $\omega$  equals 1. If  $A+A$  reactions are a superposition of independent  $N+N$  collisions then  $\Phi_{p_T}(A+A) = \Phi_{p_T}(N+N)$ , whereas  $\omega(A+A) = \omega(N+N) + \langle n \rangle \omega_{\text{part}}$ , where  $\langle n \rangle$  is the mean multiplicity of hadrons from a single  $N+N$  collisions and  $\omega_{\text{part}}$  represents fluctuations in  $N_{\text{part}}$ . The above equations suggest that while  $\Phi_{p_T}$  is independent of  $N_{\text{part}}$  fluctuations,  $\omega$  is strongly dependent on them. In the NA49 fixed target experiment  $N_{\text{part}}^{\text{proj}}$  can be fixed (spectator energy measured by the Forward Calorimeter), whereas  $N_{\text{part}}^{\text{targ}}$  cannot be measured. It was shown [18] that fluctuations of  $N_{\text{part}}^{\text{targ}}$  can be suppressed only by selection of very central collisions. Therefore multiplicity fluctuations are presented ( $\omega$ ) for very central (1%) collisions.

Figures 7, 8, 9, and 10 present energy ( $\mu_B$ ) dependence and system size ( $T_{\text{chem}}$ ) dependence of  $\Phi_{p_T}$  and  $\omega^3$ . The chemical freeze-out parameters,  $T_{\text{chem}}(A, \sqrt{s_{NN}})$  and  $\mu_B(A, \sqrt{s_{NN}})$  were taken from fits with the hadron gas model [1] to particle yields. The lines correspond to predictions for CP<sub>1</sub> and CP<sub>2</sub> (Fig. 6) with estimated magnitude of the effects for  $\Phi_{p_T}$  and  $\omega$  at CP<sub>1</sub> and CP<sub>2</sub> taken from Ref. [12,20] assuming correlation lengths  $\xi$  decreasing monotonically with decreasing system size: (a)  $\xi(\text{Pb} + \text{Pb}) = 6$  fm and  $\xi(p+p) = 2$  fm (dashed lines) or (b)  $\xi(\text{Pb} + \text{Pb}) = 3$  fm and  $\xi(p+p) = 1$  fm (solid lines). The expected magnitudes include NA49 corrections due to limited rapidity range (forward-rapidity) and limited azimuthal angle acceptance. The width of the enhancement in the  $(T, \mu_B)$  plane due to the CP is based on Ref. [21] and taken as  $\sigma(\mu_B) \approx 30$  MeV and  $\sigma(T) \approx 10$  MeV.

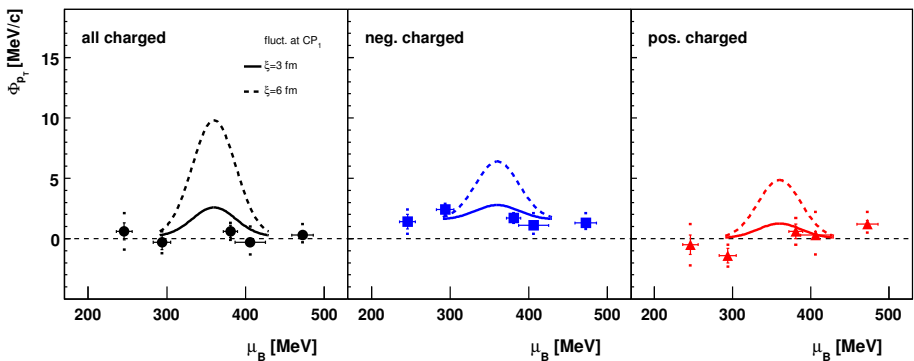


Fig. 7. Energy dependence of  $\Phi_{p_T}$  for 7.2% most central Pb + Pb collisions [15]. Lines correspond to CP<sub>1</sub> predictions (see text); their base-lines are the mean  $\Phi_{p_T}$  values for 5 energies.

<sup>3</sup> All  $\Phi_{p_T}$  and  $\omega$  values presented here are obtained in the forward-rapidity region and in a limited azimuthal angle acceptance (see corresponding papers for details).

Figures 7 and 8 show no significant energy dependence of  $p_T$  and multiplicity fluctuations at SPS energies. Thus, the results do not provide evidence for critical point fluctuations, but a narrower  $\mu_B$  scan would be desirable. Figures 9 and 10 present the system size dependence and show a maximum of  $\Phi_{p_T}$  and  $\omega$  for C + C and Si + Si interactions at the top SPS energy. The peak is twice higher for all charged than for negatively charged particles as expected for the critical point [12]. Both figures suggest that the NA49 data are consistent with the CP<sub>2</sub> predictions.

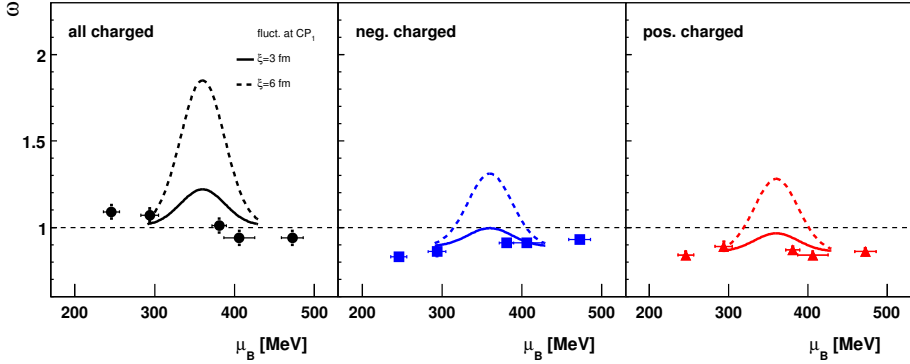


Fig. 8. Energy dependence of  $\omega$  for 1% most central Pb + Pb collisions [17]. Lines correspond to CP<sub>1</sub> predictions (see text); their base-lines are the mean  $\omega$  values for 5 energies.

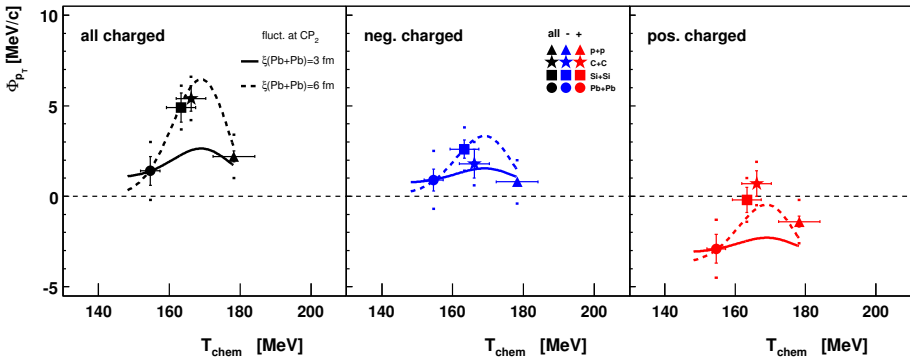


Fig. 9. System size dependence of  $\Phi_{p_T}$  at 158 A GeV with  $p+p$ , semi-central C + C (15.3%) and Si + Si (12.2%), 5% most central Pb + Pb [14]. Lines correspond to CP<sub>2</sub> predictions (see text) shifted to reproduce the  $\Phi_{p_T}$  value for central Pb + Pb collisions.

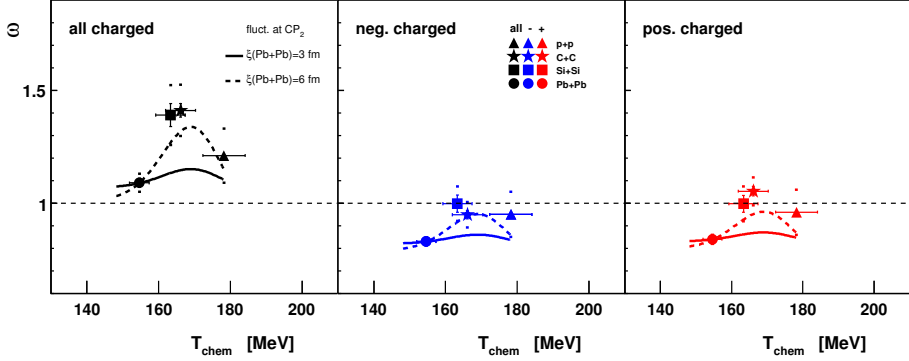


Fig. 10. System size dependence of  $\omega$  at 158 A GeV for 1% most central  $p + p$  [16], C + C and Si + Si [19], and Pb + Pb [17]. Lines correspond to  $CP_2$  predictions (see text) shifted to reproduce the  $\omega$  value for central Pb + Pb collisions.

It was expected that fluctuations due to the CP originate mainly from low  $p_T$  pions [12]. Therefore, in the NA49 analysis of  $\Phi_{p_T}$  the standard  $p_T$  range ( $0.005 < p_T < 1.5$  GeV/ $c$ ) was divided into two separate  $p_T$  regions:  $0.5 < p_T < 1.5$  GeV/ $c$  and  $0.005 < p_T < 0.5$  GeV/ $c$ . Indeed, the high  $p_T$  region shows fluctuations consistent with zero (see conference slides or Ref. [22]) and correlations are observed predominantly at low  $p_T$  (Fig. 11). However, in the low  $p_T$  region, data do not show a maximum, but a continuous rise towards Pb + Pb collisions. The origin of this behavior is currently being analyzed (short range correlations are considered).

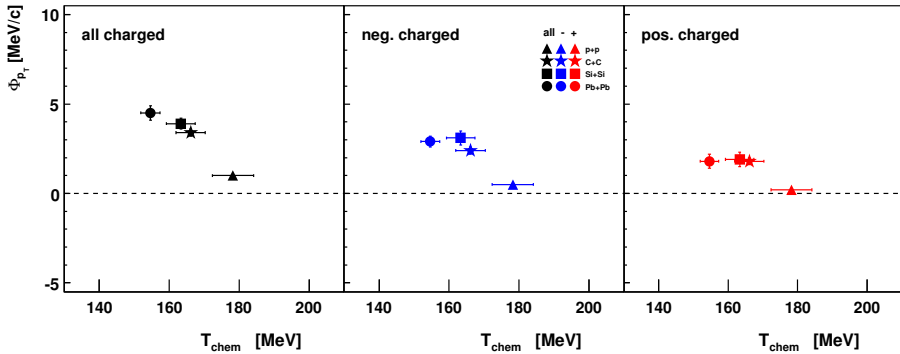


Fig. 11. The same as Fig. 9 but low  $p_T$  region shown ( $0.005 < p_T < 0.5$  GeV/ $c$ ).

## 5. Summary of NA49 results and NA61/SHINE project

The NA49 experiment obtained numerous interesting results related to both the onset of deconfinement and to the critical point. Indications for the onset of deconfinement are seen in the energy dependence of the pion yield

per wounded nucleon  $N_W$  (kink), of the  $\langle K^+ \rangle / \langle \pi^+ \rangle$  ratio and  $E_s$  (horn), and of the mean transverse mass or inverse slope parameters of  $m_T$  spectra (step) in central Pb + Pb collisions at lower SPS energies (30 A GeV). The results are not reproduced by hadron-string models (RQMD, UrQMD, HSD). Extension of the HGM fits the trend of the  $\langle K^+ \rangle / \langle \pi^+ \rangle$  ratio but relies on unmeasured hadronic states and educated-guess assumptions on the branching ratios. Also the energy dependence of event-by-event hadron ratio fluctuations shows interesting effects in the lower SPS energy range (increase of  $\sigma_{\text{dyn}}(K/\pi)$  and sign change of  $\sigma_{\text{dyn}}(K/p)$ ), but their relation to the onset of deconfinement is not clear. Other (not shown) observables were examined for signatures of the onset of deconfinement: a minimum of sound velocity at low SPS energies as expected for a 1st order phase transition [23], azimuthal correlations and disappearance of near-side correlations [24]. An additional energy and system-size scan is important to search for the onset of deconfinement in collisions of light nuclei. This is the purpose of the NA61/SHINE experiment [25] at the CERN SPS.

NA49 also searched for indications of the critical point. There are no indications of the CP in the energy dependence of multiplicity and mean  $p_T$  fluctuations in central Pb + Pb collisions. Other (not shown) observables were studied: ratios of the anti-baryon/baryon transverse mass spectra and elliptic flow  $v_2$ . Neither shows indications of CP [13]. However, the system size dependence of mean  $p_T$  and multiplicity fluctuations at 158 A GeV shows a maximum in the complete  $p_T$  range (consistent with CP<sub>2</sub> predictions) and an increase from  $p + p$  up to Pb + Pb collisions in the low  $p_T$  region. The low  $p_T$  region will be carefully analyzed for the effects of short range correlations on  $\Phi_{p_T}$  and  $\omega$ . A detailed energy and system-size scan is necessary to establish the existence of the critical point. Therefore, the CP search will be continued by the NA61/SHINE experiment.

The NA61/SHINE<sup>4</sup> experiment (Fig. 12) is the successor of NA49. The main detector components are inherited from NA49. Several upgrades were already completed or are planned in the future: (a) in 2007 a forward ToF wall was constructed to extend ToF acceptance for particles with  $p < 3 \text{ GeV}/c$ , (b) in 2008 the TPC read-out and Data Acquisition system were upgraded to increase the event recording rate by a factor of  $\approx 10$ , (c) in 2011 the NA49 Forward Calorimeter will be replaced by the Projectile Spectator Detector (PSD) with a five times better resolution. This excellent resolution (about one nucleon in the studied energy range) is crucial especially for the analysis of multiplicity fluctuations.

---

<sup>4</sup> SHINE — SPS Heavy Ion and Neutrino Experiment.

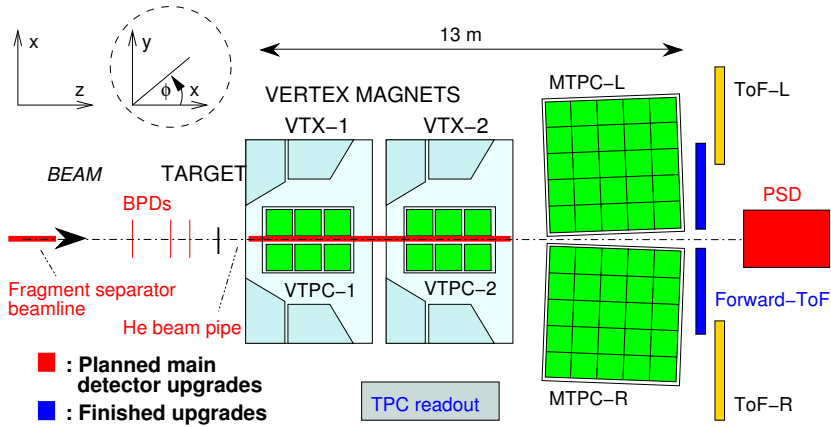


Fig. 12. The NA61/SHINE setup [25] (color on-line).

In the NA61/SHINE experiment hadron production in  $p + p$ ,  $p + A$ ,  $h + A$ , and  $A + A$  reactions at various energies will be analyzed. A broad experimental program is planned: search for the critical point, study of the properties of the onset of deconfinement, high  $p_T$  physics (energy dependence of the nuclear modification factor), and analysis of hadron spectra for the T2K neutrino experiment and for the Pierre Auger Observatory and KASCADE cosmic-ray experiments. Within the NA61/SHINE ion program we plan, for the first time in history, to perform a 2D scan with system size and energy. The future data on  $p + p$  (2009–2010; data taking in progress),  $^{11}\text{B} + ^{12}\text{C}$  (2010–2013),  $^{40}\text{Ar} + ^{40}\text{Ca}$  (2012), and  $^{129}\text{Xe} + ^{139}\text{La}$  (2014) will allow to cover a broad range of the phase diagram (see Fig. 6). With these data we will be able to:

1. Study the properties of the onset of deconfinement. In principle one can search for the onset of the ‘horn’, ‘kink’, ‘step’ in collisions of light nuclei (the structures observed for  $\text{Pb} + \text{Pb}/\text{Au} + \text{Au}$  should vanish with decreasing system size);
2. Search for the critical point. An increase of the critical point signal, the so-called hill of fluctuations, is expected for systems freezing-out near the critical point. Therefore non-monotonic dependence of the CP signal on control parameters (energy, centrality, ion size) can help to locate the critical point.

The NA61 program will be complemented by the efforts of other international and national laboratories, BNL RHIC ( $5 < \sqrt{s_{NN}} < 39$  GeV), JINR NICA ( $3 < \sqrt{s_{NN}} < 9$  GeV), GSI SIS-100(300) ( $2.3 < \sqrt{s_{NN}} < 8.5$  GeV) and by the heavy ion program at the CERN LHC ( $\sqrt{s_{NN}} = 5500$  GeV and  $\sqrt{s} = 14000$  GeV for  $p + p$ ).

## REFERENCES

- [1] F. Beccatini, J. Manninen, M. Gazdzicki, *Phys. Rev.* **C73**, 044905 (2006).
- [2] Z. Fodor, S.D. Katz, *J. High Energy Phys.* **0404**, 050 (2004).
- [3] S. Afanasiev *et al.* [NA49 Collaboration], *Nucl. Instrum. Methods* **A430**, 210 (1999).
- [4] M. Gazdzicki, M. Gorenstein, *Acta Phys. Pol. B* **30**, 2705 (1999).
- [5] C. Alt *et al.* [NA49 Collaboration], *Phys. Rev.* **C77**, 024903 (2008).
- [6] L. Kumar *et al.* [STAR Collaboration], [arXiv:0812.4099](https://arxiv.org/abs/0812.4099) [nucl-ex].
- [7] A. Andronic, P. Braun-Munzinger, J. Stachel, *Nucl. Phys.* **A772**, 167 (2006).
- [8] A. Andronic, P. Braun-Munzinger, J. Stachel, *Acta Phys. Pol. B* **40**, 1005 (2009).
- [9] M. Gorenstein *et al.*, *Phys. Lett.* **B567**, 175 (2003).
- [10] Y. Hama *et al.*, *Braz. J. Phys.* **34**, 322 (2004).
- [11] T. Schuster *et al.* [NA49 Collaboration], *PoS CPOD2009*, 029 (2009) and references therein.
- [12] M. Stephanov, K. Rajagopal, E.V. Shuryak, *Phys. Rev.* **D60**, 114028 (1999).
- [13] K. Grebieszko *et al.* [NA49 Collaboration], *Nucl. Phys.* **A830**, 547 (2009) [[arXiv:0907.4101](https://arxiv.org/abs/0907.4101)] [nucl-ex] and references therein.
- [14] T. Anticic *et al.* [NA49 Collaboration], *Phys. Rev.* **C70**, 034902 (2004).
- [15] T. Anticic *et al.* [NA49 Collaboration], *Phys. Rev.* **C79**, 044904 (2009).
- [16] C. Alt *et al.* [NA49 Collaboration], *Phys. Rev.* **C75**, 064904 (2007).
- [17] C. Alt *et al.* [NA49 Collaboration], *Phys. Rev.* **C78**, 034914 (2008).
- [18] V. Konchakovski *et al.*, *Phys. Rev.* **C73**, 034902 (2006) and private communication.
- [19] B. Lungwitz, PhD thesis (2008), <https://edms.cern.ch/document/989055/1>
- [20] M. Stephanov, private communication.
- [21] Y. Hatta, T. Ikeda, *Phys. Rev.* **D67**, 014028 (2003).
- [22] K. Grebieszko *et al.* [NA49 and NA61 Collaborations], [arXiv:0909.0485](https://arxiv.org/abs/0909.0485) [hep-ex].
- [23] V. Friese *et al.* [NA49 Collaboration], *Nucl. Phys.* **A830**, 159 (2009) [[arXiv:0908.2720](https://arxiv.org/abs/0908.2720)] [nucl-ex].
- [24] M. Szuba *et al.* [NA49 Collaboration], [arXiv:0907.4403](https://arxiv.org/abs/0907.4403) [nucl-ex].
- [25] <https://na61.web.cern.ch/na61/xc/index.html>